Early assessment of nonalcoholic fatty liver disease using multiparametric ultrasound imaging

Lokesh Basavarajappa [1], Shreya Reddy [1], Haowei Tai [2], Jane Song [1], Girdhari Rijal [3], Kevin J. Parker [4], Kenneth Hoyt [1,5]

[1] Department of Bioengineering, University of Texas at Dallas, Richardson, TX, USA
[2] Department of Electrical and Computer Engineering, University of Texas at Dallas, Richardson, TX, USA
[3] Department of Medical Laboratory Sciences and Public Health, Tarleton State University, Fort Worth, TX, USA
[4] Department of Electrical and Computer Engineering, University of Rochester, Rochester, NY, USA
[5] Department of Radiology, University of Texas Southwestern Medical Center, Dallas, TX, USA

***Abstract*—Nonalcoholic fatty liver disease (NAFLD) is the most common cause of liver disease. Patients can be characterized on the NAFLD spectrum by the progressive presence of hepatic steatosis, inflammation, hepatocyte ballooning, and then fibrosis. Currently, liver biopsy remains the only test available to detect the histologic features of NAFLD, but it is limited by its invasiveness, proneness to sampling error, and potential complications. There is an ongoing clinical need for the capability to noninvasively detect, accurately stage, and reliably monitor NAFLD. The objective of this research project was to introduce a multiparametric ultrasound (mpUS) imaging approach and evaluate its use for assessing NALFD, thereby introducing a surrogate biomarker comparable to liver biopsy. The novel method combines contrast-enhanced ultrasound (CEUS), shear wave elastography (SWE), and H-scan ultrasound (US) imaging. This approach integrates information related to liver tissue perfusion, viscoelasticity, and US scatterer size. Using Sprague-Dawley rats that were fed either control or a methionine and choline deficient (MCD) diet ($N = 6$ per group), mpUS imaging was performed at week 0 (baseline), 2 and 6. Thereafter, animals were euthanized and livers excised for histological processing and analysis. *In vivo* mpUS results from control and diet fed animals revealed that all parametric measures were statistically different at 6 weeks. Histological results revealed the presence of steatosis and mild fibrosis in animals fed the MCD diet. Overall, mpUS imaging was shown to be a promising approach for the early assessment of NAFLD.**

Keywords—contrast-enhanced ultrasound, fatty liver disease, H-scan ultrasound, shear wave elastography, tissue characterization.

I. INTRODUCTION

Nonalcoholic fatty liver disease (NAFLD) is the most common cause of liver disease among adults in the United States and affects between 80 to 100 million [1]. NAFLD comprises a wide spectrum of liver pathology ranging from non-alcoholic steatohepatitis (NASH), that can develop into liver fibrosis, cirrhosis, and hepatocellular carcinoma (HCC) [2]. Liver biopsy is commonly used as the reference standard method to grade liver cell injury from NASH [3]. However, liver biopsy is invasive, associated with sampling errors, interrater and intrarater variability, and it can lead to serious complications including bleeding and sometimes death [4].

Tested noninvasive imaging methods for NAFLD grading include magnetic resonance elastography (MRE) and magnetic resonance imaging-derived proton density fat fraction (MRI-PDFF). MRE provides a quantitative measure of liver stiffness, which is based on an analysis of shear waves induced in the liver by low-frequency vibrations applied to the abdominal wall. Measurements have been shown to correlate with fibrosis stage [5]. MRI-PDFF is a quantitative imaging biomarker of steatosis that can accurately estimate liver fat content [6]. Despite strengths, these techniques may not be practical or cost-effective for clinical screening for early stage NAFLD. On the other hand, ultrasound (US) has evolved as a promising and cost-effective imaging method for early steatosis grading [7], [8].

Ultrasound is one of the most commonly used modalities in hospitals. Technological advances in US include use of microbubbles for contrast-enhanced US (CEUS) imaging and sensitized investigation of blood flow and volume [9]–[11]. Shear wave elastography (SWE) is another US-based modality that gives insight into the viscoelastic (i.e. biomechanical) properties of soft tissue including measures of shear wave attenuation (SWA, viscosity) and shear wave speed (SWS, elasticity) [12]–[14]. A more recent innovation is H-scan US imaging, which is a tissue characterization strategy that provides information on relative US scatterer size such as cellular and tissue structures [15], [16]. Each of these US imaging modes give unique insight into select characteristics of NAFLD However, we hypothesize that a multiparametric US (mpUS) imaging method incorporating all three modes could help identify early stage NASH where medical intervention and diet modification can help reverse disease progression. Similar strategies have indeed confirmed that a mpUS strategy improves NAFLD classification compared to any one of the US modes used alone [17], [18].

In this paper, we introduce a novel mpUS strategy and image-derived biomarkers of liver tissue from use of an animal model of NAFLD. These *in vivo* mpUS measurements were optimized for preclinical studies and are linked to biophysical models of NAFLD progression [19]. For reasons partially detailed above, our unique mpUS approach combined CEUS, SWE, and H-scan US imaging.

978-1-7281-5448-0/20/$31.00 ©2020 IEEE

II. MATERIALS AND METHODS

A. Animal Preparation

Animal experiments were approved by the Institutional Animal Care and Use Committee (IACUC) at the University of Texas Dallas. Sprague-Dawley rats (Charles River Laboratories, Wilmington, MA) were randomly divided into two groups: control and diet ($N = 6$ per group). Control animals were fed standard chow, whereas diet animals were fed a special methionine and choline deficient (MCD) chow known to induce NAFLD. Before imaging, the abdomen and surrounding area were shaved with electric clippers and depilated (Nair, Church & Dwight Co, Ewing, NJ). During all procedures, animals were controlled using isoflurane anesthesia and placed on a heating pad to help maintain core body temperature.

B. mpUS Imaging

In vivo mpUS imaging of the liver in all animals occurred at baseline and again after 2 and 6 weeks of feeding with the control or MCD diet. SWE was performed using a Vantage 256 US system (Verasonics Inc, Kirkland, WA) equipped with an L11-4v linear array transducer. The SWE pulse sequence consisted of 3 rapid push beams applied using a pulse frequency of 5.2 MHz, aperture size of 64 elements, pulse length of 230 μs, and axial spacing between push beams of 2 mm. After inducing shear wave propagation in the liver parenchyma, ultrafast plane wave imaging was used to track the shear wave propagation (frame rate of 10 kHz). A 2D algorithm was used to estimate tissue displacements from the beamformed in-phase quadrature (IQ) data [20]. Thereafter, a 2D Fourier transform was applied on the tissue displacements to estimate SWS and SWA.

H-scan US imaging was performed using a Vevo 3100 system (FUJIFILM VisualSonics Inc, Toronto, Canada) equipped with an MX201 linear array transducer (center frequency of 15 MHz). Beamformed radiofrequency (RF) data was collected in the liver parenchyma and processed using a pair of convolution filters constructed using Gaussian-weighted Hermite polynomial functions of order 2 and 8 (denoted GH_2 and GH_8, respectively) [21]. The relative strength of these filter outputs was normalized by the signal energy $\sqrt{E_n}$ and then the lower frequency backscattered US signals (GH_2) were assigned a red (R) channel and higher frequency components (GH_8) to a blue (B) channel. The envelope of the original unfiltered data was assigned to a green (G) channel to complete the RGB color map and H-scan image display. H-scan US image intensity was calculated as a ratio of the B channel to the sum of the R and B channel components and describes relative scatterer size (rSS).

CEUS was also performed using the Vevo 3100 US system but in a MB-sensitive nonlinear imaging mode (center frequency of 12.5 MHz). After administering a slow bolus injection of MB contrast agent via a place tail vein catheter (50 μL; Definity, Lantheus Medical Imaging, N Billerica, MA), a temporal sequence of CEUS image were acquired (about 1 min). After placement of a region-of-interest (ROI) in the liver parenchyma or circumscribing the inferior vena cava (IVC), a mean time-intensity curve was constructed. From each, the peak enhancement (PE) and wash-in rate (WIR) parameters were extracted and represent surrogate measurements of blood volume and flow rate, respectively. CEUS parameters from the liver parenchyma were normalized by those from the IVC. Note that CEUS image was performed last in the mpUS sequence as the presence of any residual MBs in circulation could induce bioeffects if exposed to high-intensity US during SWE imaging.

C. Histological Analysis

Animals were humanely euthanized after 6 weeks of mpUS imaging and the livers were excised. Liver tissue was then embedded in paraffin, sectioned (5 μm), and stained with hematoxylin and eosin (H&E) or a Picro Sirius red solution (Sigma Aldrich, St. Louis, MO). Digital microscopy images were acquired for each stain and used for the identification of steatosis and fibrosis, respectively.

D. Performance Measures

All experimental data was summarized as mean ± SD. Boxplots were used to display data distributions based on median and quartile values. A two-tailed *t*-test evaluated differences between control and diet group measures. A p-value less than 0.05 was considered statistically significant. All statistical analyses were completed using Prism 8.3 (GraphPad Software Inc, San Diego, CA).

III. RESULTS

Animals fed standard chow or an MCD diet were imaged using a new mpUS approach at baseline and again at weeks 2 and 6 before euthanasia. This mpUS approach included *in vivo* measures of SWS and SWA from SWE, PE and WIR from CEUS, rSS from H-scan US, and traditional B-scan US images. Fig. 1 summarizes the progression of these US parametric estimates in rat liver throughout the study. After only 6 weeks, all US parameters from control and diet group animals were found to be significantly different ($p < 0.05$). More specifically, SWS parameters from the liver parenchyma were reduced by 26.3% (control, 1.8 ± 0.4 m/s; diet, 1.3 ± 0.2 m/s) and SWA parameters increased by 39.9% (control, 71.8 ± 16.0 Np/m; diet, 100.4 ± 20.6 Np/m). H-scan US image intensity values increased by 28.2% (control, 52.2 ± 1.0; diet, 66.9 ± 4.3) and B-scan US by 16.3% (control, 24.4 ± 0.8; diet, 28.3 ± 0.4). Lastly, the PE was reduced by 50.6% (control, 0.4 ± 0.2; diet, 0.2 ± 0.1) and WIR by 78.7% (control: 0.4 ± 0.2, Diet: 0.1 ± 0.1). After termination at week 6, livers were excised and processed using standard histological techniques, Fig. 2. The representative liver image from an animal fed the MCD diet reveals considerable formation of steatosis and mild fibrosis, which was not present in any of the control liver tissue. These patterns were consistent in all histology sections.

IV. DISCUSSION

Accurate detection of liver fat and fibrosis content is highly important for the evaluation of NAFLD stages. MRE provides liver stiffness measurements that correlate with fibrosis stage [5]. MRI-PDFF is another useful imaging tool that can accurately determine the amount of fat in the liver and helps in the quantification of steatosis [6]. Although these techniques provide accurate measurements, one of the major criticisms with

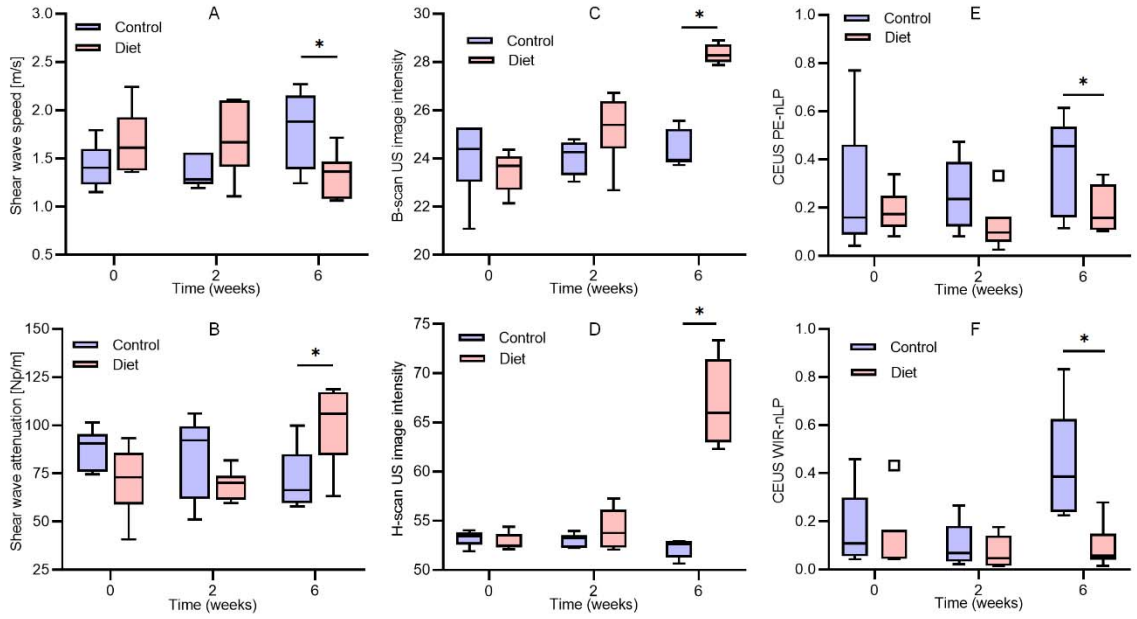

Fig. 1. Summary of *in vivo* multiparametric ultrasound (mpUS) liver measurements from rats fed standard or a methionine and choline deficient (MCD) diet for 6 weeks. Shown are boxplots for the following measures: (A) Shear wave speed, (B) shear wave attenuation, (C) B-scan ultrasound (US) image intensity, (D) H-scan US image intensity, (E) contrast-enhanced US (CEUS)-derived peak enhancement (PE), and (F) CEUS-derived wash-in rate (WIR) in the liver parenchyma (LP) normalized by like parametric measures from the inferior vena cava (IVC). A * denotes a p-value < 0.05.

MRE and MRI-PDFF assessments is the high cost associated with MRI scanners along with the technical expertise required to perform and interpret readings.

US is an alternative imaging method for early screening of NAFLD. Steatosis can be classified using B-mode US images and the assessment of liver echogenicity that is linked to fat accumulation. However, B-mode US has relatively poor interobserver agreement due to its subjective nature, along with reduced sensitivity in detecting mild hepatic steatosis. In recent years, several different US biomarkers have been developed assess a range of soft tissue properties. In this study, we introduced a new mpUS method that uses SWE parameters to access liver viscoelasticity, CEUS to capture features of liver vascularity, and H-scan US to obtain tissue microstructure information.

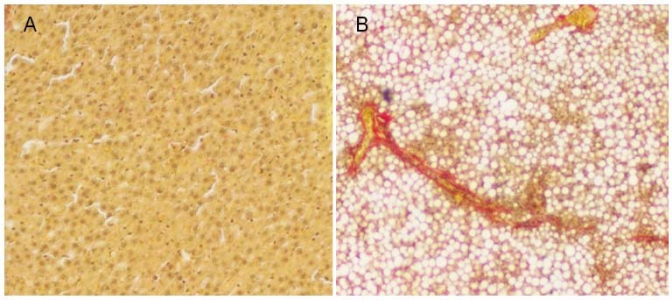

Fig. 2. Representative histological sections of liver tissue from animals fed the (A) control or (B) MCD diet at 6 weeks. Note the pressence of steatosis (white circular voids) and slight fibrosis (red) in the diet fed animal livers.

SWE is a noninvasive imaging technique that uses both US and low-frequency elastic waves to quantify biomechanical parameters related to the tissue microenvironment. In particular, the SWS is a well-studied parameter related to tissue stiffness and reveals the progression of fibrosis [14], [22], [23]. The SWA parameter is related to tissue viscoelastic loss and it increases with liver fat content, which helps assess the presence of steatosis [13], [24], [25]. CEUS uses MB contrast agents that are confined to the vascular space to improve visualization of blood flow and measurement of tissue perfusion kinetics. It is now known that fat accumulation affects vascularity in the liver parenchyma. A recent study has demonstrated that CEUS imaging was more sensitive in quantifying fatty liver disease progression with an accurate determination of NASH in a mouse model [9]. Lastly, backscattered US signals have been analyzed to obtain the microstructural properties of liver tissue. The main objective is to find hidden patterns in the US data to reveal more information about liver tissue pathology that cannot be seen in the more traditional US images [17], [18]. In this current study, we used the newer H-scan format for the classification of US scatterers [26]–[28]. Herein we showed that progression of NAFLD alters the H-scan US signal and reflects liver pathology like microvesicular steatosis.

V. CONCLUSIONS

Experimental results from animals fed a standard or MCD diet showed that all *in vivo* mpUS measurements were

significantly different by 6 weeks. Further, these US imaging results were qualitatively confirmed by histological findings that revealed the MCD fed animals had considerable levels of steatosis. Future work will examine the mpUS data classification accuracy and a more detailed comparison to histological measurements. Overall, mpUS imaging is a promising approach for the early assessment of NAFLD.

REFERENCES

[1] J. D. Browning *et al.*, "Prevalence of hepatic steatosis in an urban population in the United States: impact of ethnicity," *Hepatology*, vol. 40, no. 6, pp. 1387–1395, 2004.

[2] L. A. Adams, P. Angulo, and K. D. Lindor, "Nonalcoholic fatty liver disease," *CMAJ*, vol. 172, no. 7, pp. 899–905, 2005.

[3] S. McPherson, T. Hardy, E. Henderson, A. D. Burt, C. P. Day, and Q. M. Anstee, "Evidence of NAFLD progression from steatosis to fibrosing-steatohepatitis using paired biopsies: implications for prognosis and clinical management," *J Hepatol*, vol. 62, no. 5, pp. 1148–1155, 2015.

[4] D. E. Kleiner *et al.*, "Design and validation of a histological scoring system for nonalcoholic fatty liver disease," *Hepatology*, vol. 41, no. 6, pp. 1313–1321, 2005.

[5] S. Jayakumar *et al.*, "Longitudinal correlations between MRE, MRI-PDFF, and liver histology in patients with non-alcoholic steatohepatitis: Analysis of data from a phase II trial of selonsertib," *J Hepatol*, vol. 70, no. 1, pp. 133–141, 2019.

[6] B. Wildman-Tobriner *et al.*, "Association between magnetic resonance imaging-proton density fat fraction and liver histology features in patients with nonalcoholic fatty liver disease or nonalcoholic steatohepatitis," *Gastroenterology*, vol. 155, no. 5, pp. 1428–1435, 2018.

[7] A. Ozturk *et al.*, "Quantitative hepatic fat quantification in non-alcoholic fatty liver disease using ultrasound-based techniques: A review of literature and their diagnostic performance," *Ultrasound Med Biol*, vol. 44, no. 12, pp. 2461–2475, 2018.

[8] L. Castera, M. Friedrich-Rust, and R. Loomba, "Noninvasive assessment of liver disease in patients with nonalcoholic fatty liver disease," *Gastroenterology*, vol. 156, no. 5, pp. 1264–1281, 2019.

[9] H. Pandit *et al.*, "Utilizing contrast-enhanced ultrasound imaging for evaluating fatty liver disease progression in pre-clinical mouse models," *Ultrasound Med Biol*, vol. 45, no. 2, pp. 549–557, 2019.

[10] M. Mahoney, A. Sorace, J. Warram, S. Samuel, and K. Hoyt, "Volumetric contrast-enhanced ultrasound imaging of renal perfusion," *J Ultrasound Med*, vol. 33, no. 8, pp. 1427–1437, 2014.

[11] D. Ghosh *et al.*, "Super-resolution ultrasound imaging of skeletal muscle microvascular dysfunction in an animal model of type 2 diabetes," *J Ultrasound Med*, vol. 38, no. 5, pp. 2589–2599, 2019.

[12] K. J. Parker, A. Partin, and D. J. Rubens, "What do we know about shear wave dispersion in normal and steatotic livers?" *Ultrasound Med Biol*, vol. 41, no. 5, pp. 1481–1487, 2015.

[13] A. K. Sharma *et al.*, "Attenuation of shear waves in normal and steatotic livers," *Ultrasound Med Biol*, vol. 45, no. 4, pp. 895–901, 2019.

[14] K. R. Nightingale *et al.*, "Derivation and analysis of viscoelastic properties in human liver: Impact of frequency on fibrosis and steatosis staging," *IEEE Trans Ultrason Ferroelectr Freq Control*, vol. 62, no. 1, pp. 165–175, 2015.

[15] M. Khairalseed, K. Hoyt, J. Ormachea, A. Terrazas, and K. J. Parker, "H-scan sensitivity to scattering size," *J Med Imaging*, vol. 4, no. 4, p. 043501, 2017.

[16] M. Khairalseed, K. Javed, G. Jashkaran, J.-W. Kim, K. J. Parker, and K. Hoyt, "Monitoring early breast cancer response to neoadjuvant therapy using H-scan ultrasound imaging: Preliminary preclinical results," *J Ultrasound Med*, vol. 38, no. 5, pp. 1259–1268, 2019.

[17] E. Franceschini *et al.*, "Quantitative ultrasound in ex vivo fibrotic rabbit livers," *Ultrasound Med Biol*, vol. 45, no. 7, pp. 1777–1786, 2019.

[18] A. Tang, F. Destrempes, S. Kazemirad, J. Garcia-Duitama, B. N. Nguyen, and G. Cloutier, "Quantitative ultrasound and machine learning for assessment of steatohepatitis in a rat model," *Eur Radiol*, vol. 29, no. 5, pp. 2175–2184, 2019.

[19] K. J. Parker, J. Ormachea, M. G. Drage, H. Kim, and Z. Hah, "The biomechanics of simple steatosis and steatohepatitis," *Phys Med Biol*, vol. 63, no. 10, p. 105013, 2018.

[20] T. Loupas, R. B. Peterson, and R. W. Gill, "Experimental evaluation of velocity and power estimation for ultrasound blood flow imaging, by means of a two-dimensional autocorrelation approach," *IEEE Transactions on Ultrasonics, Ferroelectrics, and Frequency Control*, vol. 42, no. 4, pp. 689–699, 1995.

[21] M. Khairalseed, K. Brown, K. J. Parker, and K. Hoyt, "Real-time H-scan ultrasound imaging using a Verasonics research scanner," *Ultrasonics*, vol. 94, pp. 28–36, 2019.

[22] L. Gerber *et al.*, "Assessment of liver fibrosis with 2-D shear wave elastography in comparison to transient elastography and acoustic radiation force impulse imaging in patients with chronic liver disease," *Ultrasound Med Biol*, vol. 41, no. 9, pp. 2350–2359, 2015.

[23] G. Ferraioli, P. Parekh, A. B. Levitov, and C. Filice, "Shear wave elastography for evaluation of liver fibrosis," *J Ultrasound Med*, vol. 33, no. 2, pp. 197–203, 2014.

[24] C. T. Barry *et al.*, "Shear wave dispersion in lean versus steatotic rat livers," *J Ultrasound Med*, vol. 34, no. 6, pp. 1123–1129, 2015.

[25] C. T. Barry *et al.*, "Shear wave dispersion measures liver steatosis," *Ultrasound Med Biol*, vol. 38, no. 2, pp. 175–182, 2012.

[26] M. Khairalseed, F. Xiong, J.-W. Kim, R. F. Mattrey, K. J. Parker, and K. Hoyt, "Spatial angular compounding technique for H-scan ultrasound imaging," *Ultrasound Med Biol*, vol. 44, no. 1, pp. 267–277, 2018.

[27] H. Tai, M. Khairalseed, and K. Hoyt, "Three-dimensional H-scan ultrasound imaging and use of a convolutional neural network for scatterer size estimation," *Ultrasound Med Biol*, 2020 (published online).

[28] M. Khairalseed, G. Rijal, and K. Hoyt, "H-scan format for classification of ultrasound scatterers and matched comparison to histology measurements," *Proc IEEE Int Sympos Biomedical Imaging*, vol. 1, pp. 1820–1823, 2020.